Materials and Design 98 (2016) 61–67

Contents lists available at ScienceDirect

Materials and Design

journal homepage: www.elsevier.com/locate/matdes

# The comparison of microstructures and mechanical properties between 14Cr-Al and 14Cr-Ti ferritic ODS alloys

Guangming Zhang [a,b], Zhangjian Zhou [a,*], Kun Mo [c], Yinbin Miao [b,c], Shaofu Li [a], Xiang Liu [b], Man Wang [a], Jun-Sang Park [d], Jonathan Almer [d], James F. Stubbins [b]

[a] School of Materials Science and Engineering, University of Science and Technology, Beijing, Beijing 100083, China
[b] Department of Nuclear, Plasma and Radiological Engineering, University of Illinois at Urbana-Champaign, IL 61801, USA
[c] Nuclear Engineering Division, Argonne National Laboratory, Argonne, IL 60439, USA
[d] X-ray Science Division, Argonne National Laboratory, Argonne, IL 60439, USA

ARTICLE INFO

*Article history:*
Received 1 December 2015
Received in revised form 24 February 2016
Accepted 27 February 2016
Available online 3 March 2016

*Keywords:*
Synchrotron X-ray diffraction
Tensile deformation
Nanoscale particles
Microstructure

ABSTRACT

In this study, two kinds of 14Cr ODS alloys (14Cr-Al and 14Cr-Ti) were investigated to reveal the different effects between Al and Ti on the microstructures and mechanical properties of 14Cr ferritic ODS alloys. The microstructure information such as grains, minor phases of these two alloys has been investigated by high-energy X-ray diffraction and transmission electron microscopy (TEM). The in situ synchrotron X-ray diffraction tensile test was applied to investigate the mechanical properties of these two alloys. The lattice strains of different phases through the entire tensile deformation process in these two alloys were analyzed to calculate their elastic stresses. From the comparison of elastic stress, the strengthening capability of $Y_2Ti_2O_7$ is better than TiN in 14Cr-Ti, and the strengthening capability of YAH is much better than YAM and AlN in 14Cr-Al ODS. The dislocation densities of 14Cr-Ti and 14Cr-Al ODS alloys during tensile deformation were also examined by modified Williamson-Hall analyses of peak broadening, respectively. The different increasing speed of dislocation density with plastic deformation reveals the better strengthening effect of Y-Ti-O particles in 14Cr-Ti ODS than that of Y-Al-O particles in 14Cr-Al ODS alloy.



## 1. Introduction

With the improvement in safety, energetic efficiency and sustainability for advanced nuclear systems leading to higher demanding for the structural materials [1–3], the oxide dispersion strengthening (ODS) ferritic alloys have attracted increasing attentions as one of candidate materials, because of their exceptional irradiation resistance [4–6], excellent high temperature strength, and creep resistance [7,8]. The outstanding material performance stems from their unique microstructure: the highly stable nano-sized oxide particles [9,10]. It was reported that high content of chromium (>13%) in the ODS alloys is effective to suppress corrosion [11,12], while the high chromium content (>14%) can result in a thermal aging embrittlement [13,14]. Some researchers have reported the effectiveness of Al addition in ODS ferritic alloys for the improvement of corrosion resistance in Lead-cooled fast reactor (LFR) and supercritical water reactor (SCWR) [15–17]. Therefore, it is expected that an adequate combination of the Cr and Al contents will benefit for ODS ferritic alloys in the application of high temperature corrosion environment.

However, there are also some results to prove that the added Al decreased the strength of ODS alloys [15], which may be caused by the coarsed grains and different types of particles (Y-Al-O) compared with the ODS alloys without Al [18,19]. In this present study, in order to figure out the different effect of Al and Ti on the microstructures and mechanical properties of 14Cr ODS alloys. The high-energy synchrotron X-ray technique was applied to study the different responses of both matrix and nanoscale particles to externally applied stresses for 14Cr-Ti ODS and 14Cr-Al ODS alloys, respectively. The microstructure and fracture surface for these two materials were also investigated.

## 2. Materials and methods

### 2.1. Investigated materials

Nitrogen-gas-atomized powders were mixed with 0.35 wt% nano sized $Y_2O_3$ powders and 0.4 wt% titanium powders for 14Cr-Ti ODS alloys, while nitrogen-gas-atomized powders were mixed with 0.35 wt% nano sized $Y_2O_3$ powders and 4.5 wt% aluminum powders for 14Cr-Al ODS alloys. Then, two kinds of mixed powders were mechanical alloyed in a high-energy planetary ball milling with same parameters (the ball-

* Corresponding author at: Laboratory of Special Ceramics and Powder Metallurgy, School of Material Science and Engineering, University of Science and Technology Beijing, Beijing 100083, PR China.
*E-mail address:* zhouzhj@mater.ustb.edu.cn (Z. Zhou).

http://dx.doi.org/10.1016/j.matdes.2016.02.117
0264-1275/

to-powder weight ratio of 5:1, rotation speed of 300 rpm, and total milling time of 30 h) under pure argon atmosphere, respectively. Subsequently, the as-milled powders were consolidated by hot isostatic pressing (HIP) at 1150 °C under a pressure of 150 MPa for 2 h. The as-HIPed samples were forged at 1250 °C with a forging ratio of 3:1 and were then hot rolled at 1150 °C in two stages with total reduction ratio of 40%. Finally, the as-rolled samples were tempered at 650 °C for 2 h to relax the residual elastic stress. The chemical compositions of two kinds of as-rolled 14Cr ODS alloys were measured by destructive chemical analysis method. Table 1 shows the results.

### 2.2. Synchrotron WAXS investigation

The in-situ synchrotron tensile investigations were conducted at the 1-ID beamline at the Advanced Photon Source (APS), Argonne National Laboratory (ANL). The miniature tensile specimens with the gauge sections of 1.20 mm × 0.50 mm × 5.00 mm were cut from the two types of materials. The tensile tests were conducted at ambient temperature with a strain rate of $1 \times 10^{-4}$ $s^{-1}$. The X-ray scattering was performed using a monochromatic 70 keV synchrotron beam with a 300 μm × 300 μm cross-section. The Hydra detector array including four identical GE-41RT 2D detectors was used to obtain the diffraction signals, as shown in Fig. 1.

The synchrotron diffraction signals can be used to monitor the lattice strain evolution of different phases during the tensile deformation. The 15° region of the Debye-Scherrer rings near the uniaxial tensile direction and perpendicular to uniaxial tensile direction were integrated to give the lattice strains in two directions, $\varepsilon_{hkl} = (d_{hkl} - d^0_{hkl})/d^0_{hkl}$, respectively. The $d_0$ is defined as the d-spacing when elastic stress is free, which is first determined by two linear fitting on the data of two directions during the elastic deformation, and finding $d_0$ at the intersection of two fitted line. In order to minimize the effect of elastic and plastic anisotropy, the average bulk lattice strains for the ferritic matrix were calculated from the lattice strains of {110}, {200}, {211}, {310}, and {321} reflections using the weighted averaging single peaks developed by Daymond [21]. This method has been used to calculate the average bulk lattice strain for the matrix of Zircaloy-2 by averaging five Zircaloy-2 peaks [22].

$$\bar{\varepsilon} = \frac{\sum_{hkl} T_{hkl}(\theta,\psi) m_{hkl} E_{hkl} \varepsilon_{hkl}}{\sum_{hkl} T_{hkl}(\theta,\psi) m_{hkl} E_{hkl}} \tag{1}$$

where, $m_{hkl}$ is the multiplicity of the ($hkl$) reflection, $E_{hkl}$ is the Young's modulus of the ($hkl$) orientation, $\varepsilon_{hkl}$ is the lattice strain of the (hkl) reflection, and $T_{hkl}$ is the Harris texture index [23], which is defined by the following equations:

$$T(h_i) = \frac{I(h_i)/R(h_i)}{\frac{1}{n}\sum_{j=1}^{n} I(h_j)/R(h_j)} \tag{2}$$

where, $I(h_j)$ is the integrated intensity of reflection $h_j$, and $R(h_j)$ is the integrated intensity calculated from the structure factor and other parameters for a samples with a random orientation of crystallites, which has the following expression:

$$R_{hkl} = \frac{1}{V^2}\left[|F^2 p\left(\frac{1+\cos^2 2\theta}{\sin^2\theta\cos\theta}\right)\right] e^{-2M} \tag{3}$$

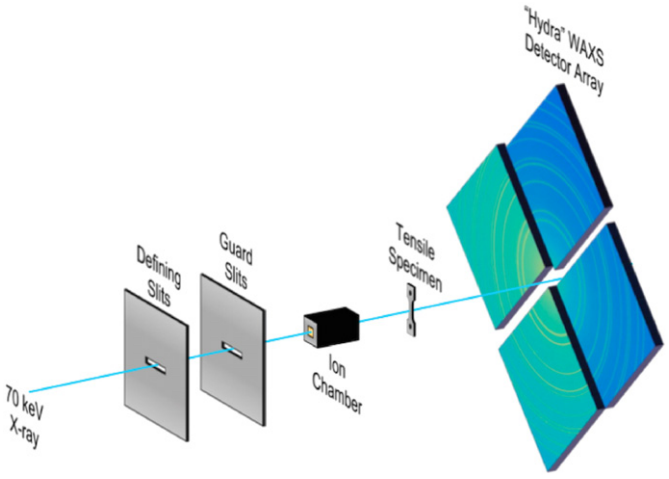


**Fig. 1.** Experimental set-up of the uniaxial tensile test with in-situ synchrotron X-ray diffraction [20].

where $V$ is the volume of the unit cell; $F$ is the structure factor; $p$ is the multiplicity of the reflection; $\frac{1+\cos^2 2\theta}{\sin^2\theta\cos\theta}$ is the Lorentz-polarization factor as a function of diffraction angle $\theta$; and $e^{-2M}$ is the temperature factor, which was calculated according to the Debye temperature and experimental temperature.

The modified Williamson-Hall (W-H) method has been applied to investigate the evolution of dislocation density in the process of tensile deformation from the synchrotron diffraction signals [24,25,20].

$$\Delta K = \frac{0.9}{D} + \left(\frac{\pi M^2 b^2}{2}\right)^{\frac{1}{2}} \rho^{\frac{1}{2}} \left(KC^{\frac{1}{2}}\right) \tag{4}$$

where $K = 2\sin\theta/\lambda$; $\Delta K = 2\cos\theta\Delta\theta/\lambda$; $\theta$ is the diffraction angle, and $\Delta\theta$ is the half of the full width at half maximum (FWHM); D is the average grain size; M is an adjustable parameter depending on the effective outer cut-off radius of dislocations, where M = 2 was used for all deformed samples [26]. $b$ is the Burgers vector of dislocations and $\rho$ is dislocation density; and C is the dislocation contrast factor, which depends on different possible combinations of Burgers vectors, line vectors of dislocations, the diffraction vector and anisotropic elastic constants [27].

### 2.3. Electron microscopy investigation

The microstructures of two materials were investigated from both thin foil samples and carbon extraction replicas using transmission electron microscopy (TEM, JEOL JEM-2100) equipped with EDS. The thin foil samples were mechanically thinned to 100 μm and punched into 3 mm discs, and then electropolished with 5% perchloric acid and 95% methanol at −20 °C using a Struer Tenupol-5 twin-jet polisher. The carbon extraction replicas were prepared from the mechanically polished surfaces. The polished surface was pre-etched by aqua regia solution (75% hydrochloric acid + 25% nitric acid) for 20 s, and then coated by a carbon film. The carbon film covering almost all of the nano-sized oxide particles were detached from matrix by electro-etching in a dilute acid solution (5% perchloric acid + 95% methanol) with a voltage of 30 V at 20 °C and then mounted on a Cu grid. Thus, the conventional TEM

**Table 1**
The chemical compositions (wt%) of the ODS ferritic alloys investigated in the present study.

| Materials | C | Cr | W | V | Si | Y | Ti | Al | O | N | S | P | Fe |
|---|---|---|---|---|---|---|---|---|---|---|---|---|---|
| Cr-Ti-ODS | 0.06 | 13.8 | 1.01 | 0.18 | 0.24 | 0.18 | 0.41 | – | 0.21 | 0.43 | 0.005 | 0.01 | Bal. |
| Cr-Al-ODS | 0.06 | 13.8 | 1.02 | 0.18 | 0.23 | 0.18 | – | 4.4 | 0.18 | 0.46 | 0.004 | 0.01 | Bal. |